



Published in final edited form as:

Pigment Cell Melanoma Res. 2015 July ; 28(4): 481–484. doi:10.1111/pcmr.12382.

ATF2 alters melanocyte response and macrophage recruitment in UV-irradiated neonatal mouse skin

Daniela Senft¹, Anabel Sorolla², Antimone Dewing¹, Giuseppina Claps¹, Eric Lau¹, Graeme J. Walker², and Ze'ev A. Ronai¹

¹Cancer Center, Sanford Burnham Medical Research Institute, La Jolla, CA, USA

²QIMR Berghofer Medical Research Institute, Herston, Australia

Dear Editor

A single exposure of melanoma-prone transgenic neonatal mice to UVB (ultraviolet B) radiation is sufficient to induce melanomas with high penetrance at an early age of onset. Although the mechanisms underlying this outcome remain elusive, the immaturity of either the melanocytes or the immune system may mediate the increased susceptibility of neonatal mice to UV-induced melanomagenesis (Wolnicka-Glubisz and Noonan, 2006). In accordance, several neonate-specific phenotypic changes mediated by UVB exposure have been reported. For example, UV irradiation of neonatal mice activates a proliferative and migratory response in melanocytes that leads to a transient increase in the number of epidermal melanocytes (Walker et al., 2009). In addition, UV irradiation results in an inflammatory response in neonates, largely characterized by macrophage infiltration (Handoko et al., 2013; Zaidi et al., 2011), which has been linked to melanomagenesis (Coleman et al., 2014; Zaidi et al., 2011). Given that ATF2, a member of the AP1 family, is a known UV-responsive transcription factor implicated in melanoma development and progression, we here analyzed the possibility that ATF2 regulates the neonatal skin response to UVB.

To test this possibility, we inactivated ATF2 in mouse melanocytes using melanocyte-Cre-induced homologous deletion of its DNA binding and leucine zipper domains (Tyr::Cre^{ERT2} mice were crossed with ATF2^{f/f} mice, referred to as ATF2⁸⁹ mice (Breitwieser et al., 2007)). When we monitored melanocyte responses to UVB irradiation administered on postnatal day (P) 4 (see Fig. 1a for a scheme of the experimental layout), we observed markedly decreased numbers of interfollicular melanocytes at 96h post UV in ATF2-mutant animals, on both C57BL/6J and FVB/N genetic backgrounds (Fig. 1b). This decrease could be attributed to: (i) differences in proliferation following UV treatment, (ii) altered apoptotic potential, or (iii) impaired migratory responses of melanocytes harboring the mutation. When we assayed proliferation (Fig. 1c) and apoptosis (Fig. 1d) of epidermal or follicular (bulb) melanocytes in response to UVB, we observed no significant differences between genotypes. Furthermore, the proliferation rate, and apoptosis, of epidermal (mainly keratinocytes) and dermal (mainly fibroblasts) cells were also similar in both genotypes (Fig. 1c and 1d, lower graphs). Together, this data suggests that, rather than influencing melanocyte proliferative or apoptotic responses; ATF2 regulates melanocyte migratory responses following neonatal UVB irradiation.

As the melanocyte response to neonatal UVB exposure was previously linked to innate immune responses (Coleman et al., 2014; Zaidi et al., 2011), we further evaluated whether melanocyte-specific expression of the ATF2-deletion mutant influences immune cell recruitment. We first performed quantitative RT-PCR for a subset of immune cell-specific transcripts in dorsal skin samples from ATF2^{WT} and ATF2⁸⁹ animals at 48h after irradiation (Fig. 2a). Levels of CD45/B220 (a B-lymphocyte marker) were similar in ATF2^{WT} and ATF2⁸⁹ skin, and whereas overall levels of CD3 (a T-cell marker) decreased compared to control samples that had not undergone irradiation, this reduction was less profound in ATF2⁸⁹ compared to wild-type skin. CD11b expression (indicative of monocytes) decreased in ATF2⁸⁹ compared to wildtype skin. Moreover, among CD11b-positive cells, expression of CD68 (a macrophage marker) was significantly decreased in ATF2⁸⁹ samples, whereas LY6G levels (a neutrophil marker) were comparable in both genotypes, suggesting decreased macrophage infiltration into skin of ATF2 mutant animals. This finding was validated by immunohistochemistry (Fig. 2b): the number of F4/80-positive macrophages in the dermis greatly increased in ATF2^{WT} animals but was notably lower in ATF2⁸⁹ mice 48 and 96h after UV exposure in mice from both a C57/BL6 and an FVB/N (measured 96h after UV) genetic background. These results support the idea that melanocytes regulate skin immune responses following UVB irradiation of neonatal mice and indicate that ATF2 functions in this activity. It remains to be determined whether ATF2 regulates the recruitment of other immune cell types (such as mast cells, eosinophils, Langerhans cells, or T-cells) and further, if these cells influence macrophage recruitment, melanocyte responses and/or melanomagenesis.

To identify signaling pathways underlying decreased melanocyte and macrophage recruitment to irradiated skin we monitored potential changes in cytokine/chemokine and growth factor expression by qRT-PCR analysis of RNA prepared from ATF2⁸⁹ or ATF2^{WT} animals 48h post irradiation. Among 24 analyzed genes (Fig. 2c) that were previously reported to be regulated following neonatal UV, we observed downregulation of CSF-1 gene expression, and (to a lesser degree) that of its receptor CSF1R, in ATF2⁸⁹ skin lysates compared to lysates from wild-type animals. CSF-1, a well-characterized macrophage growth factor, stimulates macrophage survival, proliferation, and differentiation as well as spreading and motility, and is implicated in melanoblast migration (Liao et al., 2013). In addition, ATF2⁸⁹ samples showed increased expression of CXCL10, a factor implicated in chemoattraction (Dufour et al., 2002), chemorepulsion (Kohrgruber et al., 2004), and inhibition of angiogenesis (Angiolillo et al., 1995). Increased expression of CXCL10 along with decreased expression of FGF2 transcripts in ATF2⁸⁹ relative to ATF2^{WT} samples coincided with reduced expression of both VEGF and VEGFR (Fig. 2c). Thus, ATF2-mediated signaling in melanocytes modulates the skin cytokine expression profile following UVB irradiation of neonatal mice.

Together, our data identifies a role for ATF2 in regulating melanocyte responses and has implications for innate immune responses in neonatal mice subjected to UVB irradiation. Whether the observed changes in cytokine expression are mediated directly by melanocyte ATF2 or indirectly via paracrine effects on nearby keratinocytes or fibroblasts remains to be determined. Notably, reduced macrophage density in the vicinity of melanoma has been associated with prolonged survival (Jensen et al., 2009), consistent with the oncogenic role

of ATF2 at this stage, as shown in an *Nras/Ink4a* genetic melanoma model (Shah et al., 2010). Understanding mechanisms underlying ATF2 function in melanocyte migration and macrophage recruitment should shed new light on melanoma development following exposure of neonatal mice to UVB.

References

- Angiolillo AL, Sgadari C, Taub DD, Liao F, Farber JM, Maheshwari S, Kleinman HK, Reaman GH, Tosato G. Human interferon-inducible protein 10 is a potent inhibitor of angiogenesis in vivo. *J Exp Med.* 1995; 182:155–162. [PubMed: 7540647]
- Breitwieser W, Lyons S, Flenniken AM, Ashton G, Bruder G, Willington M, Lacaud G, Kouskoff V, Jones N. Feedback regulation of p38 activity via ATF2 is essential for survival of embryonic liver cells. *Genes Dev.* 2007; 21:2069–2082. [PubMed: 17699753]
- Coleman DJ, Garcia G, Hyter S, Jang HS, Chagani S, Liang X, Larue L, Ganguli-Indra G, Indra AK. Retinoid-X-receptors (alpha/beta) in melanocytes modulate innate immune responses and differentially regulate cell survival following UV irradiation. *PLoS Genet.* 2014; 10:e1004321. [PubMed: 24810760]
- Dufour JH, Dziejman M, Liu MT, Leung JH, Lane TE, Luster AD. IFN-gamma-inducible protein 10 (IP-10; CXCL10)-deficient mice reveal a role for IP-10 in effector T cell generation and trafficking. *J Immunol.* 2002; 168:3195–3204. [PubMed: 11907072]
- Handoko HY, Rodero MP, Boyle GM, Ferguson B, Engwerda C, Hill G, Muller HK, Khosrotehrani K, Walker GJ. UVB-induced melanocyte proliferation in neonatal mice driven by CCR2-independent recruitment of Ly6c(low)MHCII(hi) macrophages. *J Invest Dermatol.* 2013; 133:1803–1812. [PubMed: 23321920]
- Jensen TO, Schmidt H, Moller HJ, Hoyer M, Maniecki MB, Sjoegren P, Christensen IJ, Steiniche T. Macrophage markers in serum and tumor have prognostic impact in American Joint Committee on Cancer stage I/II melanoma. *J Clin Oncol.* 2009; 27:3330–3337. [PubMed: 19528371]
- Kohrgruber N, Groger M, Meraner P, Kriehuber E, Petzelbauer P, Brandt S, Stingl G, Rot A, Maurer D. Plasmacytoid dendritic cell recruitment by immobilized CXCR3 ligands. *J Immunol.* 2004; 173:6592–6602. [PubMed: 15557149]
- Liao YH, Huang YT, Deng JY, Chen WS, Jee SH. Pulsed ultrasound promotes melanoblast migration through upregulation of macrophage colony-stimulating factor/focal adhesion kinase autocrine signaling and paracrine mechanisms. *Pigment Cell Melanoma Res.* 2013; 26:654–665. [PubMed: 23725022]
- Shah M, Bhoumik A, Goel V, Dewing A, Breitwieser W, Kluger H, Krajewski S, Krajewska M, Dehart J, Lau E, et al. A role for ATF2 in regulating MITF and melanoma development. *PLoS Genet.* 2010; 6:e1001258. [PubMed: 21203491]
- Walker GJ, Kimlin MG, Hacker E, Ravishankar S, Muller HK, Beermann F, Hayward NK. Murine neonatal melanocytes exhibit a heightened proliferative response to ultraviolet radiation and migrate to the epidermal basal layer. *J Invest Dermatol.* 2009; 129:184–193. [PubMed: 18633434]
- Wolnicka-Glubisz A, Noonan FP. Neonatal susceptibility to UV induced cutaneous malignant melanoma in a mouse model. *Photochem Photobiol Sci.* 2006; 5:254–260. [PubMed: 16465311]
- Zaidi MR, Davis S, Noonan FP, Graff-Cherry C, Hawley TS, Walker RL, Feigenbaum L, Fuchs E, Lyakh L, Young HA, et al. Interferon-gamma links ultraviolet radiation to melanomagenesis in mice. *Nature.* 2011; 469:548–553. [PubMed: 21248750]

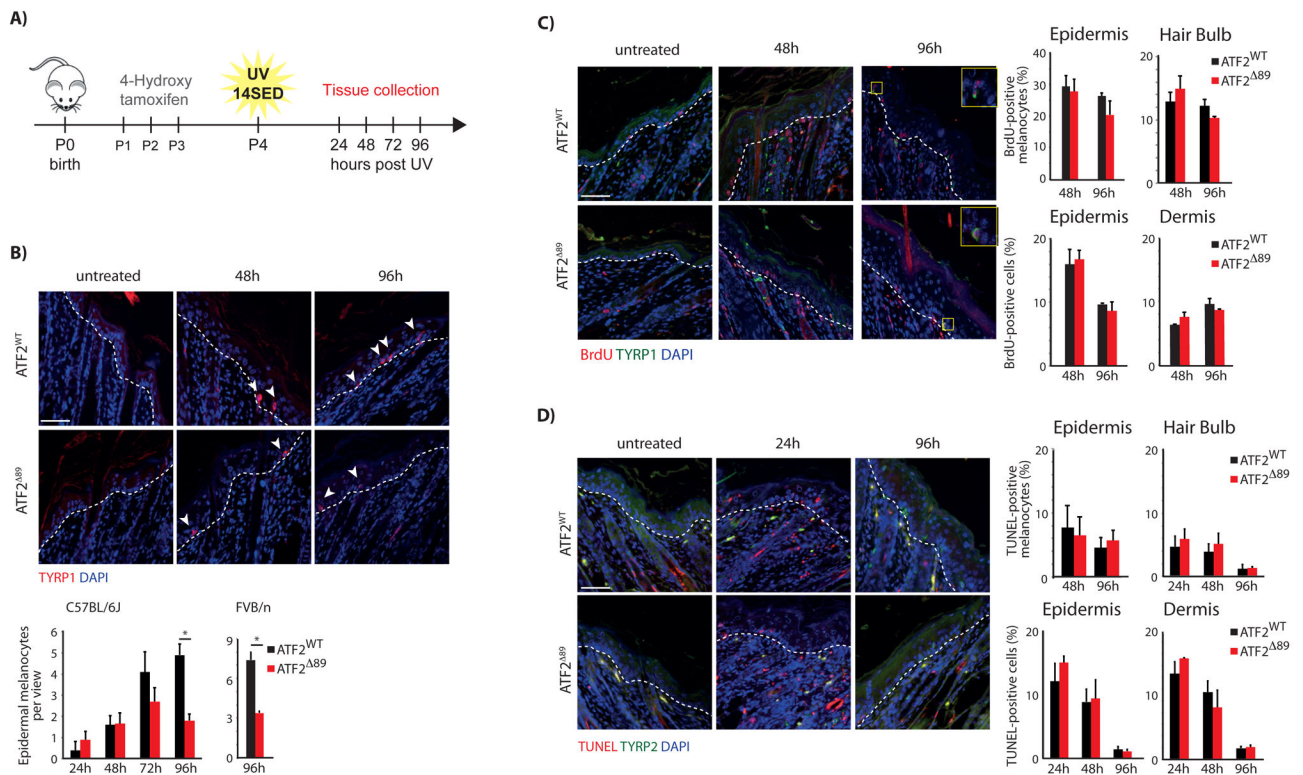


Figure 1. Decreased epidermal melanocyte count in ATF2^{Δ89} mice following neonatal UVB irradiation

A) Cartoon of the experimental layout: Pups (ATF2^{WT} x Tyr:CRE^{ERT2} and ATF2^{f/f} x Tyr:CRE^{ERT2}) were treated with 4-Hydroxytamoxifen on 3 consecutive days (P1,P2,P3) to induce melanocyte-specific CRE-excision (resulting in ATF2^{WT} and ATF2^{Δ89} mice). On P4, pups were exposed to UVB irradiation using a Black Ray lamp (FL15E, UV-320; UVP, San Gabriel, CA; emits light between 300–320nm, peaking wavelength 315nm). Exposure time was calculated using the following equation: Time (seconds) = 14 SED (J/m²)/(Non-weighted UVB dose (W/m²) x CIE_{315nm}). Standard Erythemal Dose (SED), describes the ability of a UV source to induce skin reddening; the irradiance of the UV source (Watts/m²) is weighted with the International Commission on Illumination (CIE) erythemal response function (CIE_{315nm}=0,025). Skin samples were collected at the indicated time points. Skin from non-irradiated littermates was collected as a control. **B)** Dorsal skin sections of ATF2^{WT} and ATF2^{Δ89} mice were prepared at indicated time points following UV-irradiation and stained for the melanocyte-specific protein TYRP1 (red). Shown are representative pictures of staining at indicated time points. Arrowheads indicate interfollicular melanocytes. Graphs show epidermal melanocyte number per field on C57BL/6J and FVB/N genetic backgrounds. **C)** Pups were injected intraperitoneal with 100mg/kg BrdU 3h prior to tissue collection. Proliferative cells were determined by BrdU (red) staining, and proliferative melanocytes by TYRP1 counterstaining (green); Inlays show magnified view of BrdU and TYRP1 double-positive melanocytes. Graph summarizes percentage of proliferative melanocytes (epidermis or hair bulb) and percentage of BrdU-positive epidermal or dermal cells. **D)** Representative photographs of a TUNEL assay (red) and TYRP2 staining (green)

of skin sections at indicated time points. Apoptotic cells are indicated by red staining, melanocytes by green staining. Graphs show percentage of apoptotic epidermal or bulb melanocytes or apoptotic epidermal or dermal cells. **B–D**) Epidermal:dermal junction is depicted by a dotted line in all photomicrographs. Scale bar 50 μ m. At least 3 mice per group were analyzed, and all graphs display means and SEM. Asterisks indicate significant differences, as determined by a *t*-test with $p < 0.05$.

Author Manuscript

Author Manuscript

Author Manuscript

Author Manuscript

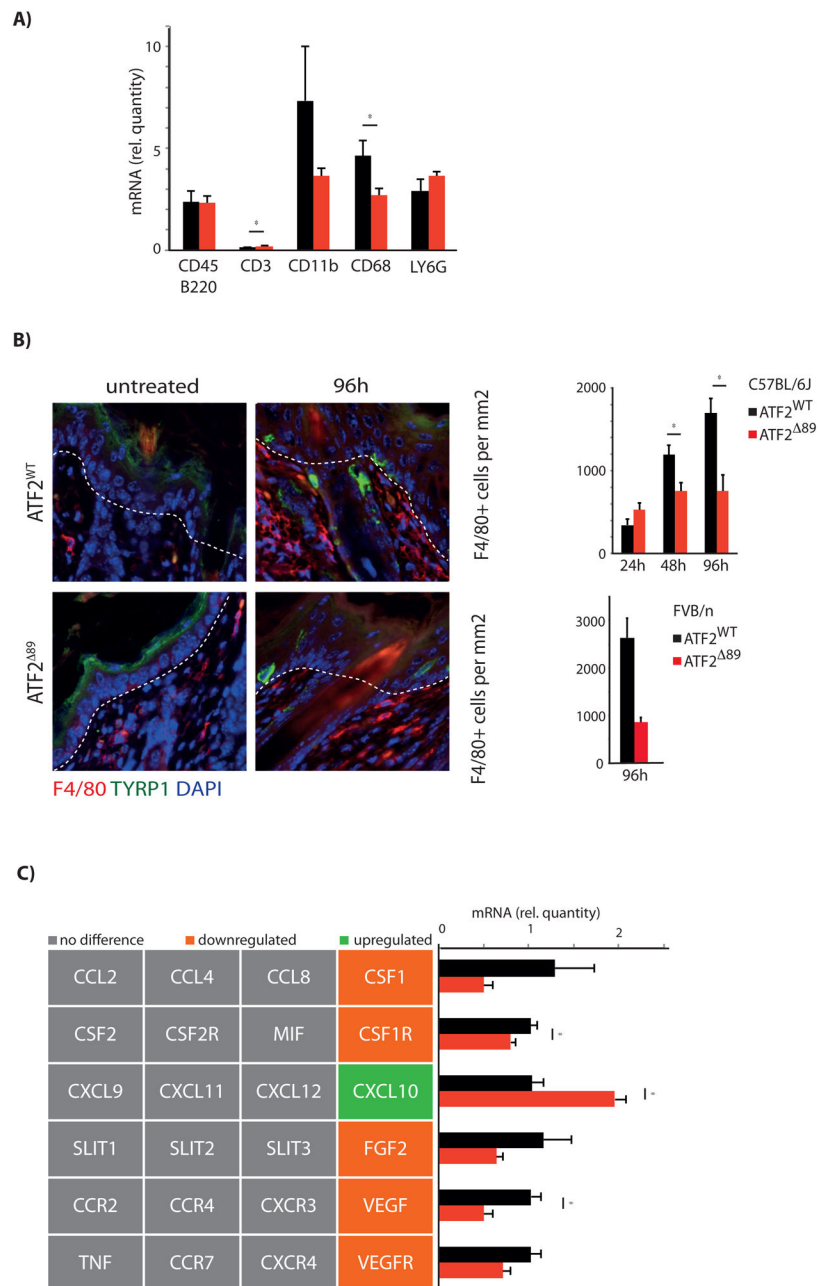


Figure 2. Analysis of immune cell infiltration into skin of ATF2^{WT} or ATF2⁸⁹ mice following exposure of neonates to UVB
A) RNA from the dorsal skin of ATF2^{WT} and ATF2⁸⁹ mice was prepared 2 days after UVB irradiation and levels of transcripts encoding immune factors (CD3, T-cells; CD45/B220, B-cells; CD11b, monocytes; CD68, macrophages; LY6G, neutrophils) were determined by qRT-PCR. **B)** Skin sections of ATF2^{WT} and ATF2⁸⁹ mice were stained for the macrophage marker F4/80 (left: representative pictures of 3 independent experiments are shown; scale bar 50µm) and macrophage infiltration into the dermis was quantified (right). **C)** RNA from the dorsal skin of ATF2^{WT} and ATF2⁸⁹ mice was prepared 2 days following UVB irradiation and levels of 24 transcripts encoding chemotactic cytokines, growth factors, and

factors implicated in angiogenesis were analyzed by qRT-PCR. Each box represents one transcript analyzed. Graphs for mRNA levels that are differentially expressed in ATF2⁸⁹ samples compared to ATF2^{WT} samples are shown next to the corresponding box; data not shown for transcripts with comparable expression level in both genotypes. **A–C)** Mean and SEM of at least 3 biological replicates are shown. Asterisks indicate significant difference as determined by a t-test with $p < 0.05$.